

EUROPHYSICS LETTERS

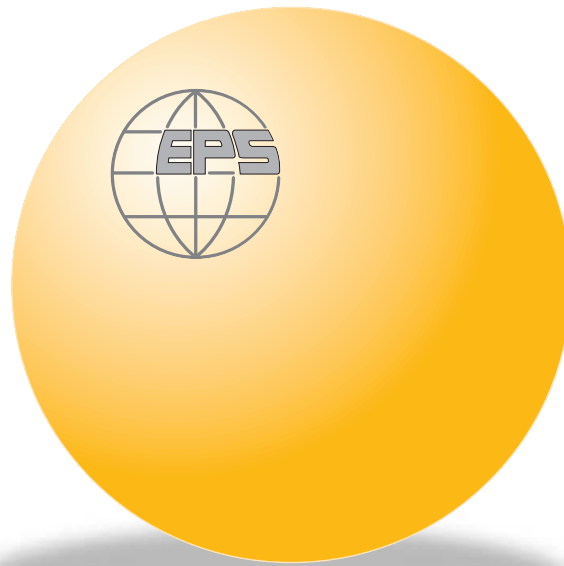
OFFPRINT

Vol. 69 • Number 5 • pp. 839–845

Monte Carlo calculations of the free-energy landscape
of vesicle formation and growth

* * *

S.-J. ZHAO and J. T. KINDT



Published under the scientific responsibility of the
EUROPEAN PHYSICAL SOCIETY
Incorporating
JOURNAL DE PHYSIQUE LETTRES • LETTERE AL NUOVO CIMENTO

Monte Carlo calculations of the free-energy landscape of vesicle formation and growth

S.-J. ZHAO and J. T. KINDT

Department of Chemistry, Emory University - Atlanta, GA, 30322, USA

received 25 August 2004; accepted in final form 7 January 2005

published online 4 February 2005

PACS. 87.16.Dg – Membranes, bilayers, and vesicles.

PACS. 87.15.Aa – Theory and modeling; computer simulation.

Abstract. – A flat-histogram Monte Carlo sampling method is used to calculate the free-energy landscape of a simple semi-flexible triangulated membrane model as a function of the number of vertices and the number of free edges. Results yield the equilibrium ratio of open (disk) and closed (vesicle) states, the free-energy barrier between these states, and the scaling of vesicle free energy with size N in the range from 6 to 200 vertices. Deviations from the predictions of a simple model for the disk-vesicle transition are found to result from the fluctuations of the edge. Vesicle free energies are fit to the form $BN + \nu k_B T \ln N$, with coefficient $\nu = 1.6 \pm 0.1$ for flexible membranes (consistent with self-avoiding branched polymer statistics) and 1.2 ± 0.1 for semiflexible membranes.

Introduction. – Self-assembled bilayer membranes have a remarkable propensity to form closed shells or vesicles. The factors governing the size distribution of these vesicles are complex. In a recent experimental study of phospholipid vesicle formation [1, 2], Leng *et al.* determine that the vesicle size distribution is determined kinetically by the minimum size at which open membrane fragments, growing as they fuse together, can rapidly make the transition to the vesicle state. In contrast, vesicles composed of fatty acids may absorb and exchange material at a high enough rate to allow observation of vesicle size distributions at equilibrium [3–5]. Depending on system properties, therefore, vesicle size distributions may be controlled by the relative free energies of (and free-energy barriers between) open (“disk”) and closed (“vesicle”) states and/or by the relative free energies of vesicles of different sizes.

Aspects of the free-energy landscape on which the disk-vesicle transition and vesicle growth occur have been previously explored. The “spherical cap” (SC) model of Fromherz [6] describes the balance between the edge energy of the disk (*i.e.* the product of the circumference of the free edge of the disk and a line tension Λ characteristic of the material) and the bending energy of the vesicle (given by $8\pi(\kappa + \frac{1}{2}\bar{\kappa})$ for any size spherical vesicle with membrane bending modulus κ and saddle-splay modulus $\bar{\kappa}$). Continuum variational calculations by Boal and Rao have shown that the SC model significantly overestimates the barrier between disk and vesicle [7]. Boal and Rao also studied fluctuation effects on the transition through Monte Carlo simulations [7], in flexible ($\kappa \leq 1.15 k_B T$) model membranes. Several theoretical efforts have been made to determine the influence of fluctuations on the vesicle free energy as a function of

size [8–10], some of which have also incorporated effects such as trans-bilayer asymmetry [11], mobile charges [12], and compositional fluctuations [13]. While many aspects of the scaling behavior of vesicles have been explored and tested by Monte Carlo simulations [14], and while self-assembly of vesicle structures has been demonstrated in a number of computer simulations [15–19], special effort is required to map out the relative free energies of states differing in topology and size.

Here we describe flat-histogram Monte Carlo sampling methods [20, 21] to calculate the free-energy landscape of a simple semi-flexible self-avoiding surface model as a function of the surface area and perimeter, encompassing disk, vesicle, and intermediate states. We find (as previously observed in flexible membrane systems [7]) that even up to a bending modulus of $k = 4.04 k_B T$, the scaling behavior of the transition is strongly influenced by shape fluctuations of the free edge. The non-linear scaling of vesicle free energy with size can be fit with a logarithmic term with prefactor $1.6 \pm 0.1 k_B T$ at low κ and $1.2 \pm 0.1 k_B T$ at higher κ .

Simulation methods. – A variant of the common tethered-sphere self-avoiding fluid random surface model [7] was used. The surface consists of hard spheres of diameter σ constrained to lie at the vertices of a triangular mesh with edge length between σ and $a\sigma$. The present results are confined to $a = 1.7$, which results in a fluid surface [22]. Each edge may belong to one or two triangles; any edge that belongs to only one triangle is termed a free edge. All free edges are constrained to form a single, continuous, non-self-intersecting ring. The potential of any structure satisfying the constraints of bonding, excluded volume, and topology is given by

$$U = \sum_j \frac{1}{2} k \theta_j^2 + \Lambda C. \quad (1)$$

The first term represents the bending energy, with the summation running over the dihedral angles of adjoining pairs of triangles. The spring constant k can be related to κ and $\bar{\kappa}$ according to the relation $\kappa = -\bar{\kappa} = k/\sqrt{3}$ [14]. For convenience in applying the flat-histogram free-energy sampling scheme, we define the line energy to be proportional to the number of free edges (C) irrespective of the lengths of those edges.

The positions, connectivity, and number N of vertices are allowed to fluctuate during the simulation. Position and connectivity fluctuations are achieved in part through translations and bond-redrawing moves [14, 23]. A small fraction (2%) of moves are vertex addition and removal attempts, biased so that growth or diminution of the structure occurs at free-edge sites. The algorithm for generating and accepting additions and removals is presented here only briefly; details will appear in a later publication. To select a position for trial insertion of a new vertex, first one segment of the free edge is chosen at random; let the endpoints of this segment be called vertex i and vertex $i + 1$. The choice of two distances in the range $[\sigma, a\sigma]$ of permitted bond-length from these vertices defines a circle perpendicular to the segment. A trial vertex located at any point on this circle can form a new triangle with vertices i and $i + 1$, defined by its angle θ made with the existing triangle belonging to these edge vertices. If the circle intersects spheres of radius equal to the maximum bond distance ($a\sigma$) centered on neighboring free-edge vertices (*e.g.*, vertices $i - 1$, $i - 2$, etc., and $i + 2$, $i + 3$, etc.), more than two bonds may be formed. For each sequential set of vertices $[i_{\min} \dots i_{\max}]$ containing i and $i + 1$, a range of angles $[\theta_{\min}, \theta_{\max}]$ is determined describing the arc of new vertex positions on the circle from which a new vertex can bond with all vertices in the set. A trial vertex position satisfying each bonding combination is chosen randomly from the corresponding angle range. After evaluation of the potential energy for the system for each bonding combination, one

configuration is selected with a probability weight proportional to

$$w_{i_{\min}, i_{\max}} = C_{\text{new}}^{-1} \left[\left(\frac{4|\mathbf{r}_{i+1} - \mathbf{r}_i|}{(a^2 - 1)^2 \sigma^4 (\theta_{\max} - \theta_{\min})} \right) \left(\frac{i_{\max} - i_{\min}}{C} \right) \right]^{-1} \exp \left[-\frac{U(i_{\min}, i_{\max})}{k_{\text{B}}T} \right]. \quad (2)$$

This is the Boltzmann weight of the configuration weighted by the inverse ratio of the probability of proposing the particular addition move in question and its reverse, removal move. The probability of the vertex, once added, being subject to a removal attempt is simply the inverse of the number C_{new} of free edges present after the addition. The first term in parentheses gives the inverse volume of the locus of points within the range $[\sigma, a\sigma]$ of vertices i and $i+1$ and the allowable angle range, and the factor $(i_{\max} - i_{\min})/C$ gives the fraction of choices of i that can give rise to the bonding combination. The total acceptance probability for the addition move is

$$\text{acc}(N \rightarrow N + 1) = \min \left[1, \lambda \exp[\beta U(N)] \sum_{i_{\min} \leq i} \sum_{i_{\max} \geq i+1} w_{i_{\min}, i_{\max}} \right], \quad (3)$$

with λ the activity of the vertex particle.

For vertex removal, first a vertex on the free edge, then one of the one or more new free edges that would be created upon removal of the vertex, is selected at random. The weight w of the existing configuration is then calculated exactly as it would be in a move directing addition of the vertex to that edge; weights for alternate, ‘‘dummy’’ configurations are also calculated in order to generate an acceptance probability that satisfies detailed balance:

$$\text{acc}(N \rightarrow N - 1) = \min \left[1, \left(\lambda \exp[\beta U(N - 1)] \sum_{i_{\min} \leq i} \sum_{i_{\max} \geq i+1} w_{i_{\min}, i_{\max}} \right)^{-1} \right]. \quad (4)$$

Structures with a minimal pore ($C = 4$) or closed vesicle states ($C = 0$) are also subject to special moves to close the pore by adding a bond or to open a pore by removing a bond at random.

The algorithm above is designed to sample a thermal ensemble of structures of a single membrane fragment at a given vertex particle activity λ . In the notation used by Glaus [24], where \mathbf{S} represents an allowed bonding topology and $\gamma(\mathbf{S})$ gives the number of free edges for that topology, the probability that the system will have N vertices and C free edges is

$$\begin{aligned} P(N, C) &= \frac{\lambda^N (N!)^{-1} \sum_{\substack{\mathbf{S}, \\ \gamma(\mathbf{S})=C}} \int d\mathbf{r}^{3(N-1)} \exp[-\beta U(\mathbf{r}^N, \mathbf{S})]}{\sum_{N=N_{\min}}^{N_{\max}} \lambda^N (N!)^{-1} \sum_{C=C_{\min}}^{C_{\max}} \sum_{\substack{\mathbf{S}, \\ \gamma(\mathbf{S})=C}} \int d\mathbf{r}^{3(N-1)} \exp[-\beta U(\mathbf{r}^N, \mathbf{S})]} = \\ &= \frac{\lambda^N q(N, C, \beta)}{\Xi(\beta, \lambda)}. \end{aligned} \quad (5)$$

For a complete sampling of a range of areas and perimeters (including the barrier region, if any, between disk and vesicle states) and determination of the complete free-energy function $F(N, C)$, the Wang-Landau [20]/extended density-of-states [21] methodology was applied to the problem. To do so, a biasing function $G(N, C)$ is added to the potential of any configuration in calculating acceptance probabilities. At the start of the simulation, $G(N, C)$ is set to a constant or to a linear function approximating $-F(N, C)$. After each MC move (successful

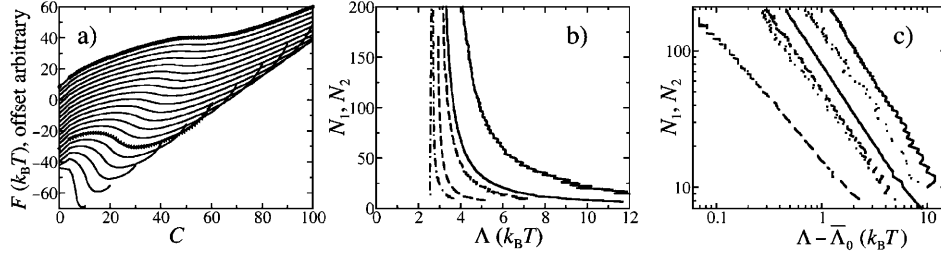


Fig. 1 – Panel (a) shows membrane free energy F as a function of number of free edges C for a system with line tension $\Lambda = 3.6 k_B T$ and $\kappa = 2.89 k_B T$ over a range of membrane sizes N from 10 (bottom) to 200 (top); only multiples of ten are shown, and curves at $N_1 = 60$ and $N_2 = 200$ are highlighted. Panel (b) shows N_1 and N_2 as functions of Λ : solid, dashed, and dot-dashed curves correspond to $\kappa = 4.04$, 1.73 , and $0.58 k_B T$, respectively; lower/left curve at each bending modulus represents N_1 and upper/right curve represents N_2 . Panel (c) shows N_1 and N_2 as functions of line tension minus the average entropy correction $\bar{\Lambda}_0 = 2.87 k_B T$ on log-log plot. Key is as in panel (b), with addition of $2.89 k_B T$ as dotted curves and omission of $\kappa = 0.58 k_B T$.

or not), the value of $G(N, C)$ for N and C corresponding to the current state of the system is raised by a small factor, which for consistency with [20] we call $\ln(f)$. A running histogram of the state (N, C) is recorded; once the histogram achieves a “flatness” criterion of values for all N, C within 20% of the mean, $\ln(f)$ is divided by two and the histogram count is restarted. In the flat histogram limit,

$$P(N, C) = \text{const} = \frac{\exp[-\beta G(N, C)] \lambda^N q(N, C, \beta)}{\Xi'(\beta, \lambda, G)}, \quad (6)$$

leading to the equality, except for a constant and a term linear in N , of the weighting function $G(N, C)$ with the negative of the free energy $F(N, C)$:

$$\beta G(N, C) = \ln q(N, C, \beta) + N \ln \lambda + \ln(\Xi/\Xi') = -F(N, C) + N \ln \lambda + \ln(\Xi/\Xi'). \quad (7)$$

Results of calculations at four values of κ are reported in the present work, each covering a range of N from 4 to 200, and a range of C between 0 and at least 70. At least 11 generations were performed for each system, reaching $\ln(f) = 10^{-4}$; four independent runs of the last generation were averaged. A generation required $\sim 10^9$ addition/removal attempts, and approximately 50 cpu-hours on a 3.0 GHz Intel Xeon processor (Penguin Computing, San Francisco, USA).

Results. – Figure 1(a) shows a series of cuts of constant membrane size N from the free-energy function $F(N, C)$ of a system with $\kappa = 2.89 k_B T$. As in the SC model [6], for any choice of bending modulus κ or line tension Λ we can identify two characteristic sizes: the lower limit N_1 of vesicle stability and the upper limit N_2 of open or “disk” state metastability. As changing line tension is a simple matter of adding a term linear in C , for a given κ we can readily determine N_1 and N_2 as functions of Λ , as shown in fig. 1(b). As noted by Boal and Rao [7], vesicles of even flexible membranes are unstable below a minimum applied line tension Λ_0 required to overcome the entropy of the edge; we estimate the true free-energetic line tension $\Lambda - \Lambda_0$ by finding the best-fit value of Λ_0 for each data set as described below.

For the most flexible membrane ($\kappa = 0.58 k_B T$), N_1 is not well defined because the vesicle state is thermodynamically stable for all sizes of membrane above a line tension of $2.4 k_B T/\sigma$,

TABLE I – Best-fit parameters for simulation data based on free-energy functions calculated at four values of bending modulus κ . Equation (8) gives definition of α_1 , $\Lambda_{0,1}$, and M_1 ; α_2 , $\Lambda_{0,2}$, and M_2 are fits to eq. (8) using $N_2(\Lambda)$ instead of $N_1(\Lambda)$. Parameters η and c are best-fit parameters to the relation $C_1 = cN_1^\eta$. B and ν are defined in eq. (9).

κ ($k_B T$)	α_1	α_2	$\Lambda_{0,1}$ ($k_B T$)	$\Lambda_{0,2}$ ($k_B T$)	M_1	M_2	η	c	ν	B ($k_B T$)
0.58	–	0.74 ± 0.07	–	2.68	–	10	0.79	1.68	1.60 ± 0.11	0.743
1.73	0.96 ± 0.10	1.2 ± 0.2	2.85	2.82	16	55	0.81	1.34	1.13 ± 0.11	1.49
2.89	1.1 ± 0.20	1.5 ± 0.4	2.86	2.25	43	285	0.75	1.43	1.24 ± 0.09	1.77
4.04	1.15 ± 0.07	1.3 ± 0.3	2.89	2.76	78	281	0.72	1.45	1.24 ± 0.14	1.95

in agreement with previous Monte Carlo study [7]. At higher κ , the trend of increasing N_1 with diminishing line tension predicted by the SC model [6] is observed, but with different scaling: instead of $N_1 \propto \Lambda^{-2}$, the best fits of $N_1(\Lambda)$ from the simulations to the form

$$N_1(\Lambda) = M_1(\Lambda - \Lambda_{0,1})^{-\alpha_1} \quad (8)$$

yield $\alpha_1 \approx 1$ over the range of systems observed (see fig. 1c and table I). A factor contributing to this discrepancy is that in-plane fluctuations of the disk edge, apparent in the typical structures shown in fig. 2, affect the scaling of perimeter (and therefore edge energy) with area. However, α_1 cannot be simply obtained as the inverse of the scaling exponent η (shown in table I) of C_1 with respect to N_1 . We thus have shown that the importance of edge fluctuation effects noted by Boal and Rao [7] persists into the regime of semiflexible membranes.

Exponents α_2 and line entropies $\Lambda_{0,2}$ were obtained from the scaling of N_2 with Λ using the form of eq. (8) and are shown in table I. The exponents range somewhat higher than α_1 (higher line tensions perhaps damping some of the edge fluctuation) but still quite lower than the zero-temperature prediction of 2. The current results show the ratio N_2/N_1 varying between 2 and 4, with the lower values associated with lower line tension. (The SC model [6] gives $A_2 = 4A_1$, while more accurate variational calculation [7] yields $A_2 \approx 1.96A_1$, for all Λ .)

In cases where vesicles can reach equilibrium through fusion, fission, or other means of exchanging material, their size distribution will be determined by their relative free energies. Unlike vesicles of an ideal, linearly elastic continuous membrane, the ground-state energy of our model vesicles shows a weak size dependence. A fit to Monte Carlo simulated annealing energies of vesicles in the range $20 \leq N \leq 100$ yielded $U_0(N) = \kappa[12.4 + 1.2 \exp[-N/21.6]]$. We obtain a ground-state energy-corrected vesicle free energy F_{corr} by subtracting U_0 from F

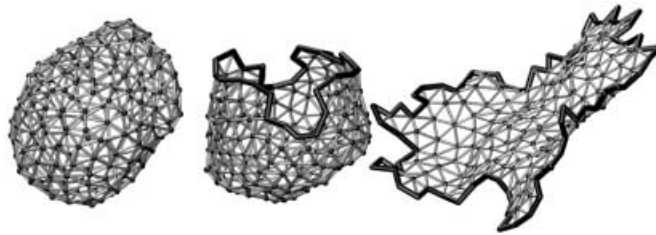


Fig. 2 – Simulation snapshots at $\kappa = 2.89 k_B T$, representing (*l-r*) vesicle, intermediate, and stable disk ($C = 0, 31$, and 77) states for $\Lambda = 3.1$, $N = N_1(\Lambda) = 200$.

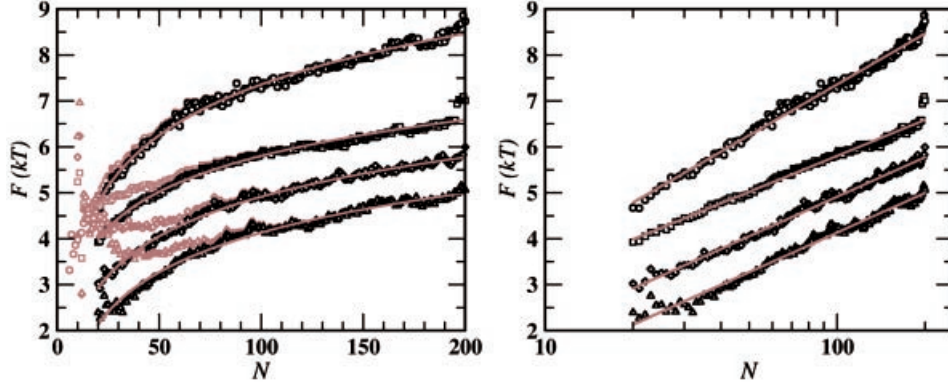


Fig. 3 – Linear (left) and log-linear (right) plots of size dependence of vesicle free energy. Symbols represent ground-state energy-corrected (black) and uncorrected (grey; red online) free energies F_{corr} and F , after subtraction of best-fit linear term BN from eq. (9). Best-fit logarithmic dependence, $\nu \ln N$ shown as grey curve. Circles: $\kappa = 0.58 k_B T$; squares: $\kappa = 1.73 k_B T$; diamonds: $\kappa = 2.89 k_B T$; triangles, $\kappa = 4.04 k_B T$. All offsets are arbitrary.

at each κ , and fit a scaling relation of the form

$$F_{\text{corr}}(N; C = 0) = BN + \nu k_B T \ln N \quad (9)$$

for $N \geq 20$. The raw data, ground-state energy-corrected data, and fits are displayed in fig. 3; best-fit parameters are shown in table I.

At $\kappa = 0.577 k_B T$, the fit with $\nu = 1.6 \pm 0.1$ agrees with the known scaling exponent of $3/2$ for self-avoiding branched polymer free energies, as previously observed in lattice studies of flexible vesicles [24]. For semi-rigid vesicles ($\kappa = 1.73, 2.89$, and $4.04 k_B T$), we see geometric “magic number” effects at $N < 20$, notably the stabilization of the icosahedral structure at $N = 12$. This regime may be relevant to self-assembly of small ordered structures, *e.g.* viral capsids [25], but not to fluid vesicles. In the range from $N = 20$ to $N = 200$ (after ground-state energy correction) we find scaling behavior independent of κ for semiflexible vesicles, with $\nu \approx 1.2 \pm 0.1$, close to the result achieved ($\nu = 1$) by substituting an effective bending modulus $\kappa_{\text{eff}} = \kappa - \alpha(8\pi)^{-1} k_B T \ln N$ for κ in calculating the energy of a spherical vesicle, using Helfrich’s [10] re-evaluated $\alpha = -1$. As such, the data appear to support the notion that fluctuations induce rigidification. However, Morse and Milner [9] have argued that this substitution neglects important long-wavelength effects, and predict $\nu = 2/3$ even assuming the original [8] and widely accepted coefficient $\alpha = 3$.

In conclusion, we have demonstrated a method to calculate the free-energy landscape governing the growth and closure of a finite self-avoiding semi-flexible model membrane. The two-dimensional landscape function gives the free-energy profile of the transition from a “disk” state with a free edge to a fully closed vesicle state. As observed by Boal and Rao [7], we see the spherical cap model to be inadequate both for its poor representation of the transition state and for its neglect of fluctuations of the disk edge. The calculated scaling of free energy with vesicle size for a flexible membrane agrees with previous lattice simulations in giving self-avoiding branched polymer-like behavior. For semiflexible vesicles, the apparent logarithmic correction to linear scaling of free energy with size has a coefficient near 1.2. Insofar as the modest size range captured represents the true scaling behavior, these results provide a direct benchmark to evaluate analytic predictions of fluctuation effects on membrane rigidity.

* * *

Support from the University Research Committee of Emory University is gratefully acknowledged.

REFERENCES

- [1] LENG J., EGELHAAF S. U. and CATES M. E., *Europhys. Lett.*, **59** (2002) 311.
- [2] LENG J., EGELHAAF S. U. and CATES M. E., *Biophys. J.*, **85** (2003) 1624.
- [3] CHEN I. A. and SZOSTAK J. W., *Biophys. J.*, **87** (2004) 988.
- [4] CHENG Z. L. and LUISI P. L., *J. Phys. Chem. B*, **107** (2003) 10940.
- [5] OLSSON U. and WENNERSTROM H., *J. Phys. Chem. B*, **106** (2002) 5135.
- [6] FROMHERZ P., *Chem. Phys. Lett.*, **94** (1983) 259.
- [7] BOAL D. H. and RAO M., *Phys. Rev. A*, **46** (1992) 3037.
- [8] HELFRICH W., *J. Phys. (Paris)*, **47** (1986) 321.
- [9] MORSE D. C. and MILNER S. T., *Phys. Rev. E*, **52** (1995) 5918.
- [10] HELFRICH W., *Eur. Phys. J. B*, **1** (1998) 481.
- [11] SAFRAN S. A., PINCUS P. and ANDELMAN D., *Science*, **248** (1990) 354.
- [12] KUMARAN V., *J. Chem. Phys.*, **99** (1993) 5490.
- [13] BERGSTRÖM M. and ERIKSSON J. C., *Langmuir*, **14** (1998) 288.
- [14] GOMPPER G. and KROLL D. M., *Phys. Rev. E*, **51** (1995) 514.
- [15] DROUFFE J.-M., MAGGS A. C. and LEIBLER S., *Science*, **254** (1991) 1353.
- [16] NOGUCHI H. and TAKASU M., *Phys. Rev. E*, **64** (2001) 041913.
- [17] YAMAMOTO S., MARUYAMA Y. and HYODO S., *J. Chem. Phys.*, **116** (2002) 5842.
- [18] DE VRIES A. H., MARK A. E. and MARRINK S. J., *J. Am. Chem. Soc.*, **126** (2004) 4488.
- [19] FARAGO O., *J. Chem. Phys.*, **119** (2003) 596.
- [20] WANG F. and LANDAU D. P., *Phys. Rev. E*, **64** (2001) 056101.
- [21] YAN Q., FALLER R. and DE PABLO J. J., *J. Chem. Phys.*, **116** (2002) 8745.
- [22] GOMPPER G. and KROLL D. M., *Phys. Rev. Lett.*, **78** (1997) 2859.
- [23] BAUMGÄRTNER A. and HO J.-S., *Phys. Rev. A*, **41** (1990) 5747.
- [24] GLAUS U., *Phys. Rev. Lett.*, **56** (1986) 1996.
- [25] BRUINSMA R. F., GELBART W. M., REGUERA D., RUDNICK J. and ZANDI R., *Phys. Rev. Lett.*, **90** (2003) 248101.